# Vegetation dynamics in the Northeastern Mediterranean region during the past 23 000 yr: insights from a new pollen record from the Sea of Marmara

V. Valsecchi, M. F Sanchez Goñi, L. Londeix

Clim. Past, 8, 1941–1956, 2012
www.clim-past.net/8/1941/2012/
doi:10.5194/cp-8-1941-2012


Climate of the Past

# Vegetation dynamics in the Northeastern Mediterranean region during the past 23 000 yr: insights from a new pollen record from the Sea of Marmara

**V. Valsecchi**[1,2,*], **M. F. Sanchez Goñi**[1], **and L. Londeix**[3]

[1]Ecole Pratique des Hautes Etudes, CNRS EPOC – UMR5805, Université Bordeaux 1, Avenue des Facultés, 33405 Talence, France
[2]Institut des Sciences de l'Evolution de Montpellier (ISEM), Département Paléoenvironnements et Paléoclimats, UMR5554, Université Montpellier 2, Bat. 22, CC061, Place Eugène Bataillon, 34095 Montpellier cedex 5, France
[3]Université Bordeaux 1, CNRS EPOC – UMR5805, Avenue des Facultés, 33405 Talence, France
[*]present address: Institut des Sciences de l'Evolution de Montpellier, Département Paléoenvironnements et Paléoclimats, UMR5554, Université Montpellier 2, Bat. 22, CC061, Place Eugène Bataillon, 34095 Montpellier cedex 5, France

*Correspondence to:* V. Valsecchi (verushka.valsecchi@univ-montp2.fr)

Received: 31 July 2012 – Published in Clim. Past Discuss.: 29 August 2012
Revised: 6 November 2012 – Accepted: 7 November 2012 – Published: 6 December 2012

**Abstract.** High-resolution pollen analysis of core MD01-2430 from the Sea of Marmara (40°47.81′ N, 27°43.51′ E) allows us to reconstruct the vegetation response to climatic changes during the past 23 cal ka in the Northeastern Mediterranean. Variation in mesic/temperate forest cover indicates major climatic shifts connected to Heinrich Stadial 1, Bölling-Allerød, Younger Dryas and to the onset of the Holocene. Pollen–anthropogenic indicator approach was used to recognize human-induced landscape changes in the Sea of Marmara. The pollen-inferred onset of the Holocene occurs at ca. 11.5 cal ka, indicating that the Northeastern Mediterranean region represents a transitional zone where higher moisture availability supported an earlier forest expansion than the borderlands of the Aegean Sea and Black Sea. Two major forest retreats occurred during the Holocene at ca. 5.5 and 2.1 cal ka. The Holocene forest setbacks are in phase with previously published alkenone-inferred sea-surface temperature decreases in the Sea of Marmara reconstructed from the same core. Our new pollen record testifies the sensitivity of Mediterranean forests to changes in moisture availability, which is driven by changes in high-latitude atmospheric processes (North Atlantic Oscillations and/or Siberian High).

## 1 Introduction

Palynological studies carried out in the Northeastern Mediterranean region have shown that the vegetation of this region was sensitive to the climatic variations of the North Atlantic high latitudes (i.e. Heinrich events and Dansgaard-Oeschger cycles) (Geraga et al., 2005; Fletcher et al., 2010a) as well as to short climatic shifts during the Holocene (Wijmstra, 1969; Roberts et al., 2001; Lawson et al., 2005; Tzedakis, 2007; Kotthoff et al., 2008a, 2011; Pross et al., 2009). Repeated forest contractions have been associated with regional sea-surface temperature cooling events probably due to the enhancement of the Siberian High (SH), (Rohling et al., 2002; Marino et al., 2009; Pross et al., 2009; Kotthoff et al., 2011), which is responsible of cold and dry spells in winter (Saaroni et al., 1996). However, despite the extensive palynological investigations carried out in Northeastern Mediterranean, the nature and timing of vegetation dynamics at the onset of the Holocene is not yet fully clarified (Tzedakis, 2007).

The Holocene reforestation in the northern border of the Aegean Sea occurs earlier (at 10.2 cal) (Kotthoff et al., 2008a) than in the Black Sea, where the establishment of forests is dated to anywhere between 9.5 and 8 cal ka (Atanassova, 2005; Mudie et al., 2007; Shumilovskikh et al., 2012). The Sea of Marmara lies in a transitional zone

between the Aegean Sea and the Black Sea and may, therefore, be a key area to clarify the timing of early Holocene reforestation in the Northeastern Mediterranean region. Moreover, no high-resolution palaeoclimatic record exists for this region displaying a direct correlation between changes in sea-surface temperatures and vegetation changes at times of rapid climatic shifts during the last deglaciation (such as Heinrich Event 1 – HE 1, the Bölling-Allerød interstadial – B/A, and the Younger Dryas – YD). The first overview of the vegetation dynamics around the Sea of Marmara for the past 33 ka was based on low-resolution pollen records that suggested colder and drier pre- and post- Last Glacial Maximum (LGM) conditions, a warm and humid early Holocene, and sustained anthropogenic impact on vegetation from 3.5 $^{14}$C kyr BP onwards (Mudie et al., 2002, 2007). Nonetheless, unfavourable climatic conditions (e.g. dry/cold episodes) were also impacting prehistoric societies causing their collapse (Weiss et al., 1993; Vermoere et al., 2002).

In this paper we present a new pollen record from the topmost 7.5 m of a sediment core (MD01-2430) collected in the Sea of Marmara, covering the past 23 cal ka. The reconstructed SST from this sedimentary sequence revealed a series of cold spells during the last 15 000 yr (Vidal et al., 2010) and a surprisingly cold B/A interstadial which is in agreement with the dinocyst record (Londeix et al., 2009). Our main goals were (i) to characterize the Northeastern Mediterranean vegetation response, tempo, and amplitude to strong and weak North Atlantic abrupt climatic changes of the last 23 000 yr, (ii) to verify the unexpected low temperature recorded during the B/A as suggested by dinocysts analysis and alkenone-inferred SST done on the same core (see for details, Londeix et al., 2009; Vidal et al., 2010), (iii) to identify vegetation dynamics and climatic conditions (i.e. precipitation regime) prevailing during the early Holocene, and (iv) to propose the most likely atmospheric situation that can explain the climatic record of the Marmara region. To address these questions, we focused our pollen analysis on obtaining a high-temporal resolution record of vegetation dynamics for the LGM, Heinrich Stadial 1 (HS 1 – $\sim$ 19–14.6 ka, Sanchez Goñi and Harrison, 2010; Stanford et al., 2011), and the Holocene, while a lower sample resolution was used during the B/A and YD.

Understanding past climatic changes and their impact on vegetation is an urgent need, considering that from climate change projections over the Mediterranean emerges a pronounced decrease in precipitation and increase in temperature especially during the summer season (Giorgi and Lionello, 2008). It is likely that such changes in the precipitation regime will have an impact on water resources and consequently biodiversity, increase in forest fires, and reduction in crop production (Alcamo et al., 2007).

## 2 Regional setting

The Sea of Marmara is 275 km long and 80 km wide and connects the Aegean Sea with the brackish Black Sea via the 70 m deep Dardanelles Strait to the south and the 40 m deep Bosphorus Strait to the north (Fig. 1). The present oceanography of the Sea of Marmara is characterized by the outflow of brackish water from the Black Sea, whereas saline bottom water flows in from the Mediterranean Sea, which results in a surface-water salinity of 20.1–24.6 psu (Ünlüata et al., 1990). Major rivers flow into the Sea of Marmara only from the south. The Kocasu River is the biggest modern river entering the southern shelf of the Sea of Marmara and it delivers about 90 % of the total suspended riverine sediment (Ünlüata et al., 1990; Çağatay et al., 2000; Kazancı et al., 2004). The Sea of Marmara is under a dry summer subtropical climate (Köppen, 1923) with a mean winter, summer, and annual temperature of 3.8 °C, 25.7, and 13.7 °C, respectively. Annual precipitation is ca. 660 mm yr$^{-1}$ (Unal et al., 2003; Kazancı et al., 2004) with most of the precipitation occurring during winter in association with the westerly depressions, while in summer the subtropical high-pressure area brings warm and dry conditions (Trewartha, 1981). In the Marmara region, the potential vegetation is the eu-Mediterranean woodland near the coast of the Sea of Marmara and euxinian-type forest inland (Zohary, 1973; Roberts and Wright, 1993). The Euxinian forest is dominated by summergreen vegetation (*Quercus* species, *Fagus orientalis*, *F. sylvatica*, *Carpinus betulus*, *C. orientalis*, and *Castanea*), *Pinus sylvestris*, and *Abies* (Zohary, 1973). The eu-Mediterranean woodland is a drought-resistant forest that extends from the coasts up to ca. 400 m elevations. The dominant species are evergreen oaks (*Quercus ilex*, *Q. coccifera*, and *Q. infectoria*), *Pinus halepensis*, *Pistacia lentiscus*, *Olea europea*, *Ceratonia siliqua*, Poaceae, and herbs. At present, the landscape is very open and intensively farmed.

## 3 Materials and methods

The core MD01-2430 (40°47.81′ N/27°43.51′ E) was retrieved during the MD123 cruise (R/V *Marion Dufresne*) in 2001 with a Calypso piston corer on the western high separating the central basin and the Tekirda basin at 580 m water depth and is 29 m long (Fig. 1) (Vidal et al., 2010). The base of the core section consists of homogeneous silty mud, gray with dark spots and thin pyrite-rich layers. A greyish-brown ash layer is present at 698–691 cm. At 350 cm a major lithologic transition corresponds to the transition from lacustrine to marine deposits. Between 320 and 230 cm a dark layer was interpreted as sapropel. A homogenous greenish silty mud characterizes the top of the sequence (Londeix et al., 2009; Vidal et al., 2010).

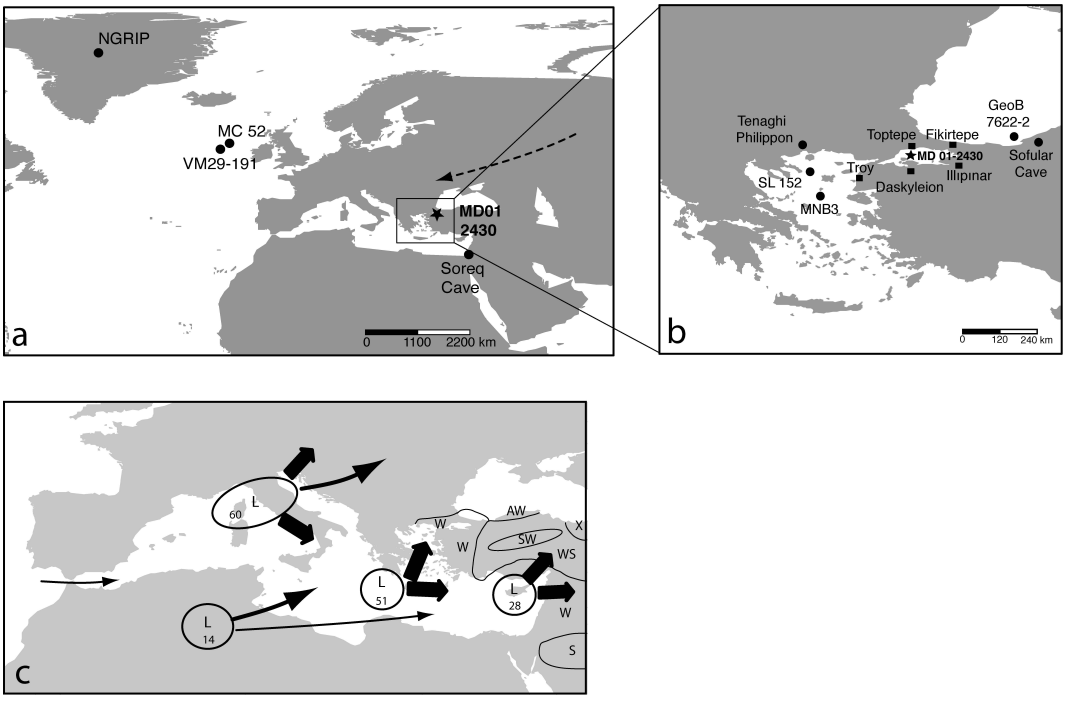


**Fig. 1.** Location of the sites discussed. **(a)** NGRIP ice core, North Atlantic (MC52 and VM29-191) and the Near East (speleothem from Soreq Cave). The dashed arrow indicates the western riding of the Siberian High during winter/spring (Marino et al., 2009). **(b)** Highlight of the sites located in Northeastern Mediterranean: sediment core in the Sea of Marmara (MD01-2430), marine cores in the Aegean Sea (SL152 and MNB3), marine core in the Black Sea (GeoB 7622-2), continental core in Greece (Tenaghi Philippon) and speleothem from Sofular Cave. Some archaeological sites are indicated by black squares. Map **(c)** indicates seasonal rainfall and the movement of depression within the Mediterranean (modify by Boucher, 1974). Seasons of maximum rainfall are shown only for Turkey and Near East: W (winter), A (autumn), S (spring) and X (indistinct). Figures in the lows indicate annual mean frequency of depressions.

### 3.1 Chronology and depth-age model

The chronology is based on six accelerator mass spectrometry radiocarbon dates on mollusc samples (Table 1, Vidal et al., 2010). Although the water reservoir age is still unknown for the Sea of Marmara, we decided to use the 400-yr correction as calculated for the Eastern Mediterranean Sea and Black Sea on modern mollusc shells (Siani et al., 2000). Indeed, the first marine incursion in the Sea of Marmara has been estimated at ca. 14.7 cal ka (Vidal et al., 2010), and after that reservoir ages in the bottom water of the Sea of Marmara are assumed to have been similar to the estimated reservoir age of the Mediterranean Sea.

Geochemistry of the ash layer deposited at 698–691 cm in core MD01-2430 confirms that it corresponds to the marine tephra Y-2. This tephra represents the distal facies of the Cape Riva eruption of Santorini, and it had been reported in other marine sediment cores from the Sea of Marmara (Çağatay et al., 2000; Wulf et al., 2002). The Cape Riva eruption has been dated on deposits on land, in which four dates have a mean value and standard deviation of $18\,310 \pm 380\,^{14}$C yr (see for details, Pichler and Friedrich, 1976; Eriksen et al., 1990; Kwiecien et al., 2008).

In order to prepare the depth-age model, the radiocarbon dates were converted to calendar years BP with the CALIB rev 5 program (Stuiver et al., 1998). We used the Marine04 calibration curve (Hughen et al., 2004) for the dates based on molluscs and the IntCal04 dataset (Reimer et al., 2004) for the Y-2 tephra age. The depth-age model was based on non-parametric weighted regression within the framework of generalised additive models (Fig. 2). The resulting model and associated age estimates and 95 % confidence intervals are based on the combined uncertainty of the calibrated dates and the regression line (Birks and Heegaard, 2003; Heegaard et al., 2005). The mean estimated ages used in this paper are slightly different from those published in Vidal et al. (2010). However, the depth-age model of Vidal et al. (2010) is within the confidence interval of our model (Fig. 2). The mean sedimentation rate during the glacial period ranges between about 70 and 30 cm kyr$^{-1}$ ($19 \pm 4$ yr cm$^{-1}$). Then during the late-glacial and early Holocene, the sedimentation rate reaches the mean lowest value of $\sim 22$ cm kyr$^{-1}$ ($46 \pm 6$ yr cm$^{-1}$). Finally, above 20 cm depth the sedimentation rate increases from 20 to 45 cm kyr$^{-1}$ ($31 \pm 15$ yr cm$^{-1}$).

**Table 1.** AMS-radiocarbon dates on core MD01-2430.

| Laboratory reference | Depth (cm) | Material dated | $^{14}$C yr BP | Reservoir correction | Calendar age cal yr BP (1 sd) |
|---|---|---|---|---|---|
| OS-35404 | 200 | *Scrobicularia plana* | $4780 \pm 55$ | 400[a] | 4952–5187 |
| OS-40506 | 253 | *Scrobicularia plana* | $8010 \pm 60$ | 400[a] | 8402–8528 |
| OS-40513 | 337 | *Arca* sp. | $10\,850 \pm 65$ | 400[a] | 12 230–12 601 |
| OS-40514 | 347 | *Arca* sp. | $11050 \pm 65$ | 400[a] | 12 657–12 803 |
| OS-40515 | 349 | *Arca* sp. | $11\,050 \pm 70$ | 400[a] | 12 647–12 807 |
| OS-40516 | 384 | *Turricaspia caspia* | $13\,050 \pm 75$ | 400[a] | 14 742–15 066 |
| Y 2/Cape Riva Tephra | 691–698 | wood | $18\,310 \pm 380$[b] | – | 21 262–22 230 |

[a] Reservoir correction following Siani et al. (2000). [b] Mean and standard deviation calculated by Kwiecien et al. (2008) based on original dating series (Pichler and Friedrich, 1976; Eriksen et al., 1990).

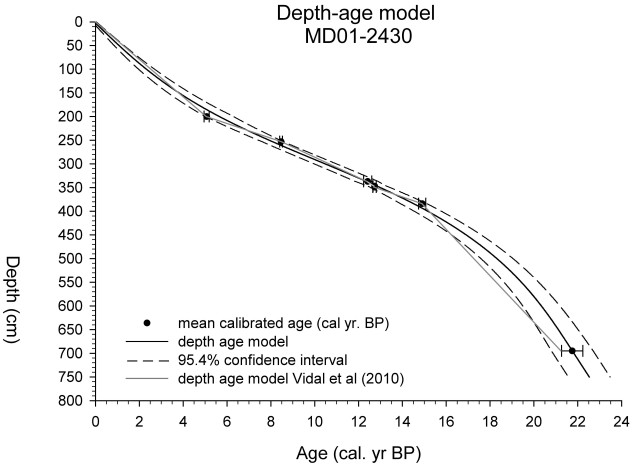


**Fig. 2.** Depth–age model (line) and 95.4 % confidence intervals (dashed lines). Calibrated radiocarbon dates are represented by dots. Depth-age model by Vidal et al. (2010) is in grey.

### 3.2 Pollen analysis

Samples of 1 cm$^3$ were used for pollen analysis, with *Lycopodium* tablets added for estimation of pollen concentration (Stockmarr, 1971). The samples were prepared as follows: coarse-sieving at 150 µm, successive treatments with cold HCl at increasing strengths (10, 25, and 50 %), successive treatments with cold HF (HF 25 % for 2 1/2 h, HF 70 % 1 1/2 days), and micro-sieving (10 µm mesh). Pollen grains and spores were counted at a magnification of $\times$ 400 and $\times$ 1000 and identified using keys, pollen atlases (Moore et al., 1991; Reille, 1992–1998), and the reference collection of the UMR EPOC, University Bordeaux 1. A minimum of 20 taxa, 100 terrestrial pollen grains (excluding *Pinus*, aquatic plants, spores, and unknown) were counted. In addition, a minimum of 200 objects (including *Lycopodium* and terrestrial pollen grains) were counted in each sample to obtain accurate concentration estimates (Finsinger and Tinner, 2005). The average terrestrial pollen sum is $160 \pm 60$ grains excluding *Pinus*, or 260 grains including *Pinus*. Pollen grains of *Pinus* are generally over-represented in marine pollen records and are therefore excluded from the pollen sum (Heusser and Balsam, 1977; Turon, 1984; Rossignol-Strick and Planchais, 1989). Rull (1987) indicated that a pollen sum of 200 grains is statistically sufficient to produce reliable estimates. Indeed, after this value there are not significant variations in the widths of confidence intervals for percentage, while for pollen counts of 100 grains the variation is of ca. 1 %. Maher (1981) showed how pollen percentages stabilize as the pollen sum increases, using the confidence intervals of the multinomial distribution. Changes in pollen percentages detected in our core are significant even considering the 0.95 confidence limits (Maher, 1981).

The pollen types are grouped as follows: steppic (Chenopodiaceae, *Artemisia*, *Ephedra distachya*, and *E. fragilis*), Mediterranean (*Quercus* evergreen type, *Olea*, *Phillyrea*, *Cistus*, and *Pistacia*), temperate (all trees and shrubs excluding *Pinus*, *Hippophaë*, *Quercus* evergreen type, *Olea*, *Phillyrea*, *Cistus* and *Pistacia*, *Ephedra distachya*, *E. fragilis*), and upland herbs. The arboreal pollen group (AP) includes Mediterranean and temperate pollen types. The program TILIA was used for plotting the pollen diagrams (Grimm, 1993). The identification of Holocene forest setbacks was based on shifts in AP percentage of at least 20 % between adjacent samples. The sample resolution of the pollen record of 3–10 cm allowed for an average time resolution of $115 \pm 100$ yr (1 standard deviation – SD) during the glacial section, $420 \pm 100$ yr for the late-glacial and $170 \pm 90$ yr for the Holocene. The pollen record was zoned using the visual zonation of the pollen curves on the basis of coincident changes occurring in multiple pollen taxa.

## 4 Results

### Vegetation dynamics inferred from the pollen analysis

The pollen zone MD30-1 (22.5–21 cal ka) was dominated by herbs (Cichorioideae, *Aster* type, and *Centaurea nigra*

type), steppic plants (*Artemisia* and Chenopodiaceae), *Hippophaë* and high pollen percentages of *Pinus* (not included in the pollen sum) (Fig. 3a). Pollen of temperate trees (mainly *Quercus* deciduous type and *Fagus*) were also present, reaching two minima at 21.7 and 21.1 cal ka. These minima correspond to an increase in *Artemisia* and Chenopodiaceae. Occurrence of reworked pollen (mainly *Carya*) most probably testifies erosion of the slope around the basin of Marmara. Important elements of the past landscape were *Hippophaë* and *Pinus* together with steppic plants, *Aster* type and Cichorioideae. At that time the water level of the Sea of Marmara was between −85 and −110 m relative to the present level and most of the shelves were exposed (Çağatay et al., 2009; Eris et al., 2011). This might have favoured *Hippophaë* and *Pinus* which are pioneer species that can grow on unstable sandy soils (Djamali et al., 2008). This type of vegetation indicates a cold and rather dry climate during a period that falls in the Last Glacial Maximum (LGM, Mix et al., 2001), as also suggested by other records from the Sea of Marmara (Mudie et al., 2007).

At the beginning of zone MD30-2 (21–19.5 cal ka), pollen percentages of temperate trees (*Quercus* deciduous type, *Fagus* and *Carpinus*) increased at the cost of upland herbs, *Hippophaë* and *Pinus* (Fig. 3a). However, the pollen influx diagram indicates that *Hippophaë* was still an important component of the landscape (Fig. 3b) and the increase in pollen percentages of temperate trees is not fully mirrored in the influx values. We can conclude that some elements of the mesic/temperate forest most probably were present in the area around the Sea of Marmara during the LGM.

In zone MD30-3 (19.5–16.6 cal ka), temperate-tree pollen percentages slightly decreased while *Artemisia*, Chenopodiaceae and Poaceae pollen values increased. This feature is mirrored in the pollen influx diagram; the landscape was then dominated by steppic plants and upland herbs. A further dominance of *Artemisia*, Chenopodiaceae, Cichorioideae and herbs is visible in zone MD30-4 (16.6–15 cal ka) and it is accompanied by increases of *Betula*, *Hippophaë* and pollen of semi-desert species (*Ephedra distachya* type and *E. fragilis* type). On the other hand, pollen percentages of *Quercus* deciduous type – *Carpinus*, *Fagus*, *Ulmus*, and *Tilia* – markedly decreased (Fig. 3a).

A sudden increase of pollen percentages of *Quercus* deciduous type characterized the zone MD30-5 (14.7–13.2 cal ka). This change is also partly reflected in the pollen influx diagram (Fig. 3b), where an increase in the influx values of *Quercus* deciduous type and disappearance of *Hippophaë* pollen indicate the establishment of a mesic/temperate forest. This vegetation shift clearly marks a change towards warmer/more humid climate. In zone MD30-6 (13.2–11.8 cal ka), increases of pollen of steppic plants (*Artemisia* and Chenopodiaceae) were paralleled by a reduction of pollen of mesic/temperate forests. Towards the end of this zone (ca. 11.8 cal ka), *Quercus* evergreen type and some temperate taxa (*Ulmus*) pollen percentages increased. The degradation of the temperate forests indicate a colder and drier climate compared to the previous pollen zone (MD30-5), which corresponds to the Younger Dryas (YD) as found in the stable oxygen isotopes in Greenland (Dansgaard et al., 1993; Rasmussen et al., 2006).

The onset of the Holocene was characterized by (i) an increase of pollen percentages of elements of mesic forests (*Quercus* deciduous type, *Fagus*, *Abies*, *Tilia*, *Ulmus*, *Carpinus*, and *Corylus*) (zone MD30-7: 12–6 cal ka), (ii) by the continuous pollen curve of *Sanguisorba minor* type since 11.5 cal ka; followed by (iii) the appearance of *Pistacia* pollen. These features are mirrored by the pollen influx values, although a sharp increase of oak pollen influx is only visible at ca. 10.5 cal ka. In this pollen zone an overall increase of the total pollen influx from two to six times corresponds to the deposition of Sapropel 1 (M1) (Fig. 3b). The occurrence of *Sanguisorba minor* type and *Pistacia* can be considered as a biostratigraphic marker for the onset of the Holocene in the Eastern Mediterranean region (Rossignol-Strick, 1995; Turner and Sánchez Goñi, 1997; Kotthoff et al., 2008a). Mesic/temperate forest is the dominant vegetation during the early-middle Holocene, characterized by *Quercus* deciduous type, *Fagus*, *Abies*, *Ulmus*, *Carpinus*, and *Corylus* pollen. This type of vegetation indicates an increase of temperature and precipitation.

During the middle-late Holocene (zones MD30-8 and MD30-9), an overall slight reduction of the mesic forest is suggested by the pollen spectra, though this type of forest was still dominant. A marked forest setback is detected at ca. 5.5 cal ka (lasted from 5.7–5.3 cal ka including two pollen samples), mainly due to a reduction of pollen percentages of *Quercus* deciduous type and increase in Poaceae and Chenopodiaceae. Then short-term minima of temperate and Mediterranean tree pollen occur at ca. 2.1 cal ka (2.5–1.7 cal ka, accounting for five pollen samples) to which correspond increases of Poaceae, Caryophyllaceae, *Sanguisorba minor* type, *Aster* type, Cichorioideae, and *Artemisia*. Increases in pollen percentage of herbs were coupled with the occurrence of anthropogenic-pollen indicators (Behre, 1990; Bottema and Woldring, 1990), such as Cerealia type, *Juglans* and *Olea* that occurred since 3.1, 2.4 and 2.3 cal ka, respectively (Fig. 5). Probably human exploitation of the mesic/temperate forest became stronger. Similarly, in other sedimentary cores from the Sea of Marmara the disappearance of *Pinus* and *Quercus* forests and the spread of *Artemisia*, Cichorioideae, and Chenopodiaceae were detected after ca. 4000 yr BP (ca. 4.3–4.8 cal ka) and attributed to the human occupation of the area around the Sea of Marmara (Mudie et al., 2002, 2007).

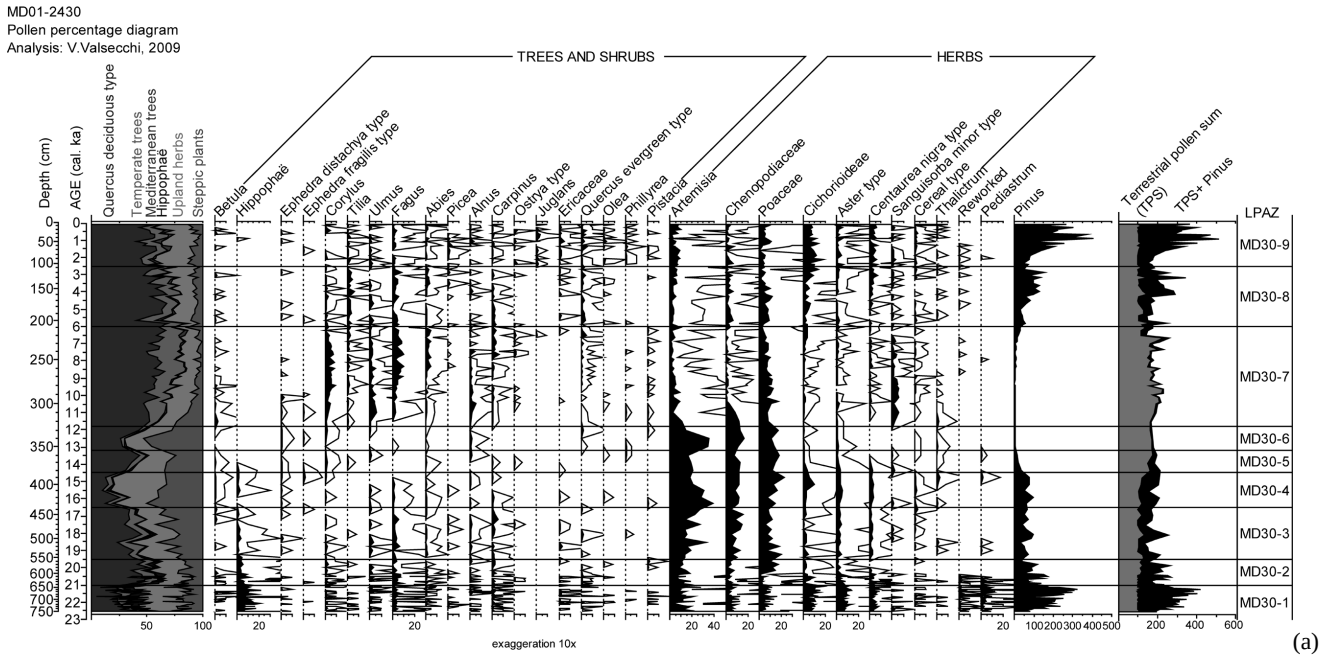


**Fig. 3. (a)** Pollen percentage diagram for core MD01-2430 showing only selected taxa. *Pinus*, aquatics, ferns and reworked pollen are not included in the pollen sum. Mediterranean trees include *Quercus* evergreen type, *Cistus*, *Olea*, *Phillyrea* and *Pistacia*. Steppic plants include *Artemisia*, Chenopodiaceae, *Ephedra distachya* type and *E. fragilis* type. Filled black curves show the percentage values of single pollen type; white curves indicate percentages enlarged by ten. **(b)** Pollen influx diagram for core MD01-2430 showing only selected taxa. Gray band indicates the Sapropel 1 (M1).

## 5 Discussion

### 5.1 Direct correlation between vegetation and sea-surface changes in the Sea of Marmara region and integration with other records from the Northeastern Mediterranean region

The beginning of the studied sequence of core MD01-2430 falls in the Last Glacial Maximum (LGM, Mix et al., 2001). The Sea of Marmara was an isolated mildly brackish (caspi-brackish) sea according with the dinocysts flora (i.e. presence of *Spiniferites cruciformis*), occurrence of *Pediastrum* and fresh-water ostracods. Occurrence of *Caspidinium rugosum* s.l. indicates influence of fresh meltwaters provided during spring. This is in agreement with $\delta^{18}$O values of benthic ostracods (Vidal et al., 2010) and with the ddominance of *Spiniferites cruciformis* that indicates a large seasonal contrast in the sea-surface temperatures (SST) (Londeix et al., 2009) (Fig. 4). Although at that time meltwaters were present, our pollen signal (excluding reworked pollen) is reflecting the terrestrial vegetation and not the possible pollen transported by river run-off. Indeed, in large lakes and marine sediments, the terrestrial vegetation nearby the coring site contributes the most to the pollen signal (Shumilovskikh et al., 2012). At that time the vegetation was dominated by *Hippophaë*, (Fig. 3a) while some peaks in *Artemisia* pollen percentages were detected, indicating short-term dry periods. An increase of thermophilic dinocysts, including subtropical/tropical coastal species and *C. rugosum* s.l., occurred between 20.6 and 18.5 cal ka, indicating presence of meltwaters (Londeix et al., 2009). At about the same time an increase in temperate pollen types (*Quercus* deciduous type, *Fagus* and *Carpinus*) and decrease in *Artemisia* is detected in the pollen diagram at 21–19.5 cal ka. Altogether these proxies indicate a change towards climatic conditions less severe than before (Fig. 4). Our data support recent model simulations for the LGM ($21 \pm 2$ ka) that indicate the potential presence of cold-tolerant species (*Carpinus*, *Corylus*, *Fagus*, *Tilia*, *Fraxinus excelsior*, *Alnus*, *Quercus robur*, and *Ulmus*) on the western shore of the Sea of Marmara (Leroy and Arpe, 2007; Arpe et al., 2011).

Arboreal pollen (AP) percentages gradually decreased starting from about 19.5 cal ka at the benefit of steppic plants (Fig. 3a). Then a minimum in AP pollen percentages was reached between ca. 17–15 cal ka; again pollen of steppic plants increased (up to 50 %) and pollen of semi-desert species (*Ephedra* sp.) were present. Similarly during this period (19.5–15 cal ka) thermophilic dinocysts almost disappeared; a first decrease is visible at ca. 18.4 cal ka and a second one at 16.4 cal ka. Cool dinocysts were present with stable values until 16.4 cal ka, when *Spiniferites cruciformis* became the dominant dynocyst (Fig. 4). The decrease in thermophilic dinocysts at 16.4 cal ka is contemporaneous with disappearance of *C. rugosum* s. l., indicating that meltwater inputs almost stopped, causing a strong reduction in SSS

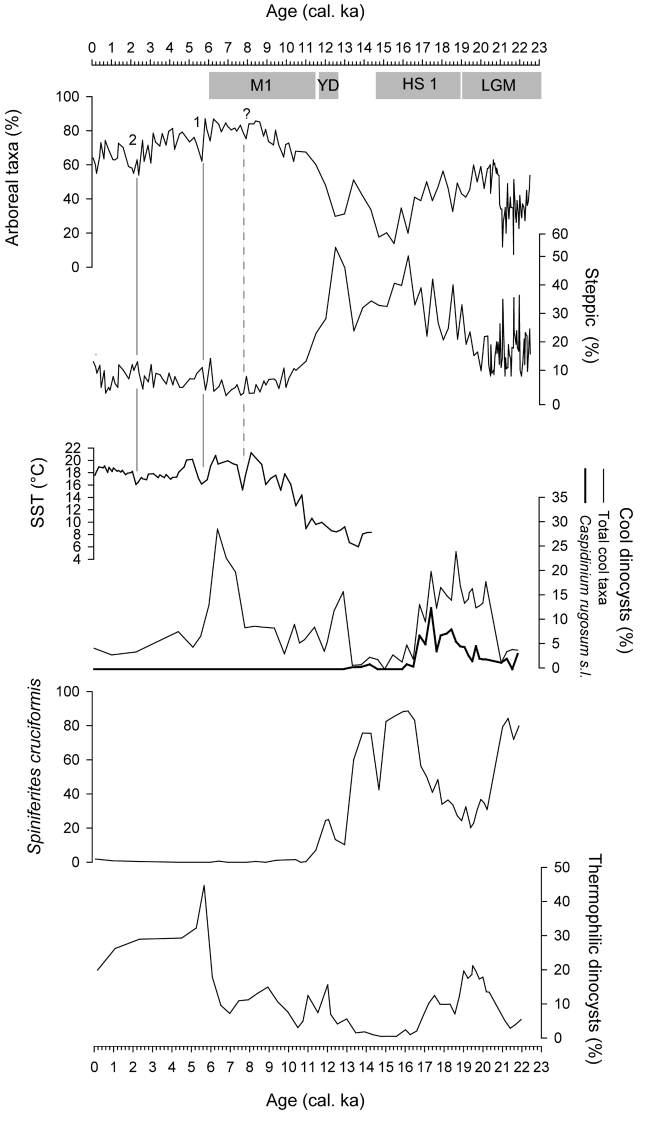


**Fig. 4.** Pollen percentages, dinocysts percentages and sea-surface temperature (SST) for core MD01-2430. Arboreal taxa include all trees and shrubs except *Hippophaë*, *Ephedra distachya* type and *E. fragilis* type. Steppic includes *Artemisia*, Chenopodiaceae, *Ephedra distachya* type and *E. fragilis* type. Alkenone derived sea-surface temperatures (SST) (Vidal et al., 2010). Thermophilic dinocysts include: *Tuberculodinium vancampoae*, *Tectatodinium pellitum*, *Spiniferites mirabilis*, *Spiniferites delicatus*, *Lingulodinium machaerophorum*, *Polysphaeridium zoharyi*, *Operculodinium israelianum*, and *Stelladinium stellatum*; cool dinocysts include: *Pentapharsodinium dalei*, *Bitectatodinium tepikiense* s.l., *Caspidinium rugosum* s.l. and *Spiniferites elongatus* s.l. (Londeix et al., 2009). Numbers 1 and 2 indicate forest setbacks. Grey boxes indicate major climatic shifts: LGM (Last Glacial Maximum) which last from 23–19 cal ka (Mix et al., 2001), HS1 (Heinrich Stadial 1) from ca. 19–15 cal ka (Sanchez Goñi and Harrison, 2010; Stanford et al., 2011), YD (Younger Dryas or GS-1) from ca. 12.7–11.7 cal ka (Steffensen et al., 2008) and M1 from ca. 7–11.5 cal ka (Vidal et al., 2010).

seasonal contrast (Londeix et al., 2009). After 16.4 cal ka, dinocyst assemblages came back to assemblages similar to those before 21 cal ka, with maybe lower SST seasonal contrast (i.e. lower summer SST) (Londeix et al., 2009). Similarly, stable oxygen isotopes indicate that the Sea of Marmara was filled with meltwaters from 23 up to 16 cal ka (Vidal et al., 2010). Increase in steppic plants (*Artemisia*) and cold dinocysts were also found in other cores from the Sea of Marmara (Mudie et al., 2007) and in the Aegean Sea (Geraga et al., 2010; Kotthoff et al., 2011), suggesting that at that time climatic conditions were more critical, e.g. colder and drier than the conditions during the LGM. Moreover, this phase can be subdivided into a first half (up to 17 cal ka) that was probably wetter than the second half (17–15 cal ka). A similar dry/cold period with a two-phase pattern was also described for the Western Mediterranean (Naughton et al., 2007; Fletcher and Sanchez Goñi, 2008; Fletcher et al., 2010a) and it was related to the HS 1, ∼19–14.6 ka (Fig. 5). Based on lake-level changes of Lake Lisan (palaeo-Dead Sea), the link between Eastern Mediterranean drought phases and HSs was present during the past 55 ka (Bartov et al., 2003). The proposed mechanism to explain this teleconnection accounts for an intensification of the Siberian High (SH), which is responsible for severe cold and dry winter conditions and polar/continental air outbreaks over the Aegean Sea (Rohling et al., 2002; Marino et al., 2009; Pross et al., 2009; Kotthoff et al., 2011). On the other hand, the collapse of the North Atlantic Deep Water circulation likely caused an input of cold water in the Mediterranean Sea and a consequent reduction in the evaporation. In turn, this would have resulted in a reduction in the strength and the frequency of storms and therefore a decrease in precipitation over the Eastern Mediterranean region (Bartov et al., 2003).

Starting from 14.7 cal ka, pollen percentages of steppic plants decreased and a sudden increase of *Quercus* deciduous type and AP is detected in the pollen record, indicating an increase in temperatures and moisture. *Spiniferites cruciformis* is still dominant (Londeix et al., 2009), indicating probable cold winters and hot summers. After 14.7 cal ka, the Sea of Marmara was influenced by both Mediterranean and Black seawaters, and alkenone-derived SST indicates low temperature most probably during spring – the period when coccoliths preferentially produce this compound (Fig. 4) (Vidal et al., 2010). A possible scenario that might explain the apparent contradiction between the climate evidence during the B/A is that the cold SST in Sea of Marmara is the result of the arrival of meltwaters; however, *C. rugosum* s.l. was not detected at that time. Another apparent contradiction is present when comparing the pollen and ostracods-derived stable-oxygen isotopes record from core MD01-2430. The isotopes show a trend towards higher values since 14.5 cal ka, which might be interpreted as an increase in evaporation. However, increase in moisture is evidenced by increase in mesic/temperate forest based on pollen data of core MD01-2430 and pollen records in the Aegean Sea (Kotthoff et al.,

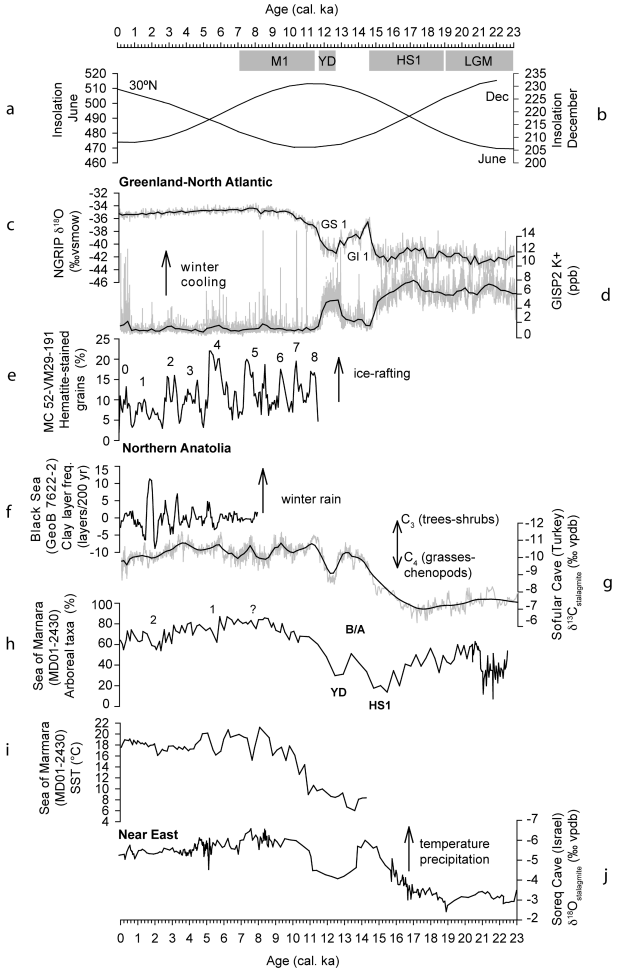


**Fig. 5.** Selected palaeoclimate records arranged by latitude (north on the top) and palaeoproxies for core MD01-2430. **(a)**–**(b)** Summer and winter insolation values at 30° N (Berger and Loutre, 1991). **(c)** NGRIP $\delta^{18}$O (‰ VSMOW) proxy for temperature based on GICC05 timescale (Andersen et al., 2006; Rasmussen et al., 2006; Vinther et al., 2006), black solid curve represents 200 years (span 0.1) running average smoothing. **(d)** GIPS2 potassium ion (ppb) proxy for the SH (Mayewski et al., 1997), black solid curve represents 200 yr (span 0.01) running average smoothing. **(e)** Ice-rafted hematite-stained grains in the North Atlantic sediment cores MC52 and VM29-191. Numbers from 0 to 8 designate the millennial-scale cycles (Bond et al., 1997, 2001). **(f)** Clay layer frequency record from core GeoB 7622-2 (Black Sea) proxy for winter precipitation in Northern Anatolia (Lamy et al., 2006). **(g)** $\delta^{13}$C (‰ VPDB) of stalagmite So-1 from Sofular Cave (Turkey) proxy for type and density of vegetation: values of −12 ‰ are characteristic for $C_3$ plants (trees and shrubs) and values of −6 ‰ for $C_4$ (grasses and chenopods) plants (Fleitmann et al., 2009), black solid curve represents 200 yr (span 0.01) running average smoothing. **(h)** Arboreal pollen type (%) including temperate and Mediterranean plants for core MD01-2430 (this study), numbers indicates forest set-backs, while labels YD, B/A and HS1 indicate biostratigraphic zone based on our data. (i) Alkenone derived sea-surface temperatures (SST) on the core MD01-2430 (Vidal et al., 2010). **(j)** $\delta^{18}$O (‰ VPDB) of Soreq Cave (Israel) (Almogi-Labin et al., 2009). Numbers 1 and 2 indicate forest setbacks **(h)**. For the legend of grey boxes LGM, HS1, YD and M1 see Fig. 5.

2008a; Kotthoff et al., 2011) and in Turkey (Jones et al., 2007). This supports the idea of Vidal et al. (2010) who attributes the increase in stable-oxygen isotopes values to the increase in precipitation-water $\delta^{18}O$ (3–4 ‰) and not to a drought phase during the B/A. A change in the seasonality of the precipitation might also explain the enrichment in the stable oxygen isotopes (Stevens et al., 2001, 2006).

In addition in our record, maximum of AP is reached towards the Allerød (Fig. 5) similarly to what was already described in Western Mediterranean (Combourieu-Nebout et al., 2009; Fletcher et al., 2010b), suggesting a warming trend from the Bölling towards the Allerød. Our findings then support the idea of a climatic contrast during B/A, with Greenland and North Europe experiencing a cooling trend towards the end of the B/A while climate stability or warming was evidenced in Southern Europe (Genty et al., 2006; Combourieu-Nebout et al., 2009).

In core MD01-2430 an optimum in dinoflagellates indicating cold conditions is again recorded between 13 and $12.15 \pm 0.25$ cal ka where *Bitectatodinium tepikiense* and *Spiniferites elongatus* are found with their highest values (Fig. 4). These species are winter cool-water indicators (Turon, 1984; Marino et al., 2009), and similarly alkenone-derived SST show low values (ca. 10 °C, Vidal et al., 2010). This is in agreement with the results of pollen analysis that indicate a withdrawal of the mesic/temperate forest and increase of steppic plants, indicating cold and dry conditions during the YD. The YD has been already described in the Northeastern Mediterranean as an abrupt event characterized by a change towards more drought-tolerant type of vegetation (Wijmstra, 1969; Rossignol-Strick, 1995; Atanassova, 2005; Lawson et al., 2005; Mudie et al., 2007; Kotthoff et al., 2008a; Shumilovskikh et al., 2012). Pollen-based climatic reconstructions for the Aegean region have also shown a decline in annual temperature of ca. 6 °C and a precipitation decrease of ca. 300 mm (Dormoy et al., 2009; Kotthoff et al., 2011) during the YD.

The onset of the Holocene in core MD01-2430 is marked by the establishment of a mesic/temperate forest with some element of the Mediterranean forest that suggests the increase in temperature and water availability. The dinocysts record shows the association of cool and thermophilic species, which might suggest a seasonal contrast in SST (Londeix et al., 2009) while SST are increasing (Fig. 4) (Vidal et al., 2010). The late-glacial/Holocene transition, as marked by the AP record, matches very well with changes in $\delta^{13}C$ values of a stalagmite located in Sofular Cave (Northwestern Anatolia) (Fleitmann et al., 2009), indicating a forested phase during the early-middle Holocene (Fig. 5). The Holocene forest setback at ca. 5.5 is directly associated with decrease in SST in the Sea of Marmara (Fig. 4), highlighting a connection between the SST, the resulting moisture availability, and changes in the forest cover. A major forest retreat at 5.6 cal ka was also found in northern borderlands of the Aegean Sea (Kotthoff et al., 2008a); similarly a decrease in SST was found in the Aegean Sea (Marino et al., 2009). At ca. 5.5 cal ka, decreases in winter–spring rain (as determined by clay layer frequency) are found in the Black Sea (Lamy et al., 2006), and a dry event is visible in stable-oxygen isotopes records of Soreq Cave (Fig. 5) (Bar-Matthews et al., 1997; Bar-Matthews and Ayalon, 2011). This drought phase coincides also with a major archaeological transition (Bar-Matthews and Ayalon, 2011; Roberts et al., 2011). Strikingly, our record shows only a weak forest retreat during the most pronounced shift in temperature at 8–7.9 cal ka as recorded by SST. Similarly, $\delta^{13}C$ of Sofular Cave does not show any marked shifts in the values around 8 cal ka (Figs. 4 and 5) (Fleitmann et al., 2007). A pronounced vegetation shift is instead detected on the northern borderland of the Aegean Sea (Kotthoff et al., 2008b) and in Tenaghi Philippon pollen records (Pross et al., 2009), which was associated with the 8.2 cal ka climate event. On the contrary, a spreading of temperate forest was recently described for the Black Sea region at ca. 8.3 cal ka and it was related to higher moisture availability (Shumilovskikh et al., 2012).

Further decreases in AP percentages from average values between adjacent samples of at least 10 % were identified at 10.4, 9.9, 9.2, 6.1, 4.3, 2.9, 2.1, 1.2 and 0.3 cal ka and interpreted as forest setbacks to which corresponds an increase of steppic plants (Fig. 5). The minor oscillations prior the human impact (ca. 2.5 cal ka) can tentatively be correlated with increases in North Atlantic ice-rafting – Bond's events (Fig. 5) (Bond et al., 1997, 2001).

### 5.2 Early Holocene moisture availability in the Sea of Marmara region

The early Holocene in our sequence is characterized by a sudden expansion of temperate trees at ca. $11.5 \pm 0.3$ cal ka (Fig. 3a), indicating an increased availability of moisture. A warm and wet early Holocene (9.5 $^{14}$C kyr BP; ca. 11 cal ka) was also invoked by Mudie et al. (2007) on the basis of pollen profiles from the Sea of Marmara. Holocene reforestation occurs at 12 cal ka in Nisi Fen (northern Greece) (Lawson et al., 2005), only at 10.2 cal ka on the northern border of the Aegean Sea according to marine pollen sequences (core SL 152, Kotthoff et al., 2008a), at ca. 8.5 $^{14}$C kyr BP ($\sim$ 9.5 cal ka) in the southwestern Black Sea (Mudie et al., 2007), at ca. 8.5 cal ka in the southeastern Black Sea (Shumilovskikh et al., 2012), and at ca. 7.1–7.5 $^{14}$C kyr BP ($\sim$ 8 cal ka) in the western Black Sea (Atanassova, 2005). However, in core SL 152 (Aegean region) a decrease in the steppic plants (*Artemisia*, Chenopodiaceae and *Ephedra*) and expansions of herbs (*Centaurea nigra* type and Cichorioideae) occurred at ca. 11.6 cal ka, indicating an increase of the water availability prior the forest expansion (Kotthoff et al., 2008a). A similar pattern can be seen in the Tenaghi Philippon sequence, where the reforestation occurs ca. 1000 yr after the decrease of the *Artemisia* and Chenopodiaceae (Pross et al., 2009).

The differing source areas for the pollen assemblages in the Sea of Marmara, Black Sea, and Aegean Sea might also explain the different timing of the reforestation. The Aegean sequence reflects the vegetation in the northern borderlands of the Aegean Sea (Kotthoff et al., 2008b), while the geographical position of the Sea of Marmara resulted in a pollen sequence that should reflect the vegetational changes on Thrace and northwestern Anatolia. The fluvial component in the Sea of Marmara is represented only by rivers that flow from the Anatolia peninsula. However, aerial pollen account for the main input in the Sea of Marmara sediments (van Zeist and Bottema, 1991; Mudie et al., 2002; Leroy et al., 2009). We can conclude that the pollen record of core MD01-2430 mainly represents northwestern Anatolia. Stable-carbon isotopes of Sofular Cave suggest a presence of forested ecosystem since 10.5 cal ka in northwestern Anatolia, indicating that during the early Holocene moisture was available and that the vegetation response to favourable climatic conditions was fast (Fig. 5) (Fleitmann et al., 2009; Göktürk et al., 2011). Conversely, a late reforestation (only after 8 ka) occurred in the drier parts of the Near East, in sites located in southernmost Europe, and in continental zones. This might be explained by a dry early Holocene where moisture levels were below the tolerance threshold for tree growth or a by a change from summer/spring to winter precipitation in sites located in Anti-Taurus-Zagros Mountains (van Zeist and Bottema, 1991; Stevens et al., 2001; Bottema and Sarpaki, 2003; Wick et al., 2003; Wright et al., 2003; Tzedakis, 2007; Djamali et al., 2010). We can conclude that the northern borderland of Southern Europe can be considered a transitional zone where the moisture level determined an earlier (ca. 11.5 cal ka) woodland expansion (e.g. Northern Anatolia as shown by our data) or a later expansion in ecological stressed areas (Tzedakis et al., 2004; Tzedakis, 2007).

The importance of the water availability (especially during winter) for the establishment of forest is highlighted by pollen-based climatic reconstructions (Kotthoff et al., 2008b; Dormoy et al., 2009). Recently, climate simulations have shown that across the early Holocene stronger winter precipitation occurred over the Northeastern Mediterranean (near Turkey), while there is little evidence for summer precipitation in the Eastern Mediterranean (Brayshaw et al., 2011). The mechanism associated with winter precipitation in Eastern Mediterranean is not yet fully understood (Giorgi and Lionello, 2008), while it has been shown that strengthening/weakening of the Indian Monsoon is related with increase/decrease in spring precipitation in Anti-Taurus-Zagros region (Djamali et al., 2010). Evidence from palaeo-data suggests that negative rainfall anomalies in the Black Sea region occurred during phases of high North Atlantic Oscillations (NAO) causing intervals of lower clay-layer frequencies (Lamy et al., 2006). A role of the Siberian High (SH), which is responsible for severe cold and dry winter conditions and polar/continental air outbreaks over the Aegean Sea (Rohling et al., 2002), is instead invoked to explain the evidence of 8.2 event in Tenaghi Philippon record (Pross et al., 2009) and centennial-scale SST cooling events in the Aegean Sea (Marino et al., 2009). Finally, comparison of palaeolimnological records from Eastern and Western Mediterranean has highlighted that NAO forcing alone cannot explain the hydrology pattern in Eastern Mediterranean since 900 AD (Roberts et al., 2012). In order to precisely establish the correlation between these two climate systems (SH/NAO) during the late-glacial and Holocene, it is necessary to make a comparison of our data with high-resolution pollen sequences from areas not affected by the SH (i.e. western part of the Mediterranean).

### 5.3 Evidences for human occupation during the Holocene

Holocene vegetation changes might be caused by variation in either climate or human activities or both. Human activities on the landscape can be detected by the increase of weeds and ruderal herbs (e.g. Chenopodiaceae, *Sanguisorba minor* type and Cichorioideae), domesticated species (e.g. Cerealia type, *Olea*, *Vitis* and *Juglans*) and an overall increase in non-arboreal pollen (NAP). However, because all these pollen types can also be present in the natural vegetation, care must be used in the interpretation of pollen diagrams of the Eastern Mediterranean (Behre, 1990; Bottema and Woldring, 1990). Although occurrence of anthropogenic-pollen indicators may be highlighted by using high pollen sums (more than 1000 grains/sample), our record shows their presence during the entire Holocene, even though their abundance changes are only visible during the Late Holocene.

Several Neolithic settlements (namely Illıpınar, Mentese, Barcın Höyük, Pendik, Fikirtepe, Yarımburkaz, and Toptepe) were established near the northern and southern shore of Sea of Marmara from ca. 8.4–7.4 cal ka (Roodenberg and Alpaslan-Roodenberg, 1999; Bottema et al., 2001; Rosenstock, 2005; Özdogan, 2011), possibly causing a change in the landscape (Fig. 1). Palaeoenvironmental investigations connected with archaeological excavations were carried out in the area around Illıpınar excavations (Fig. 1). The pollen spectra of Yenisehir core (the only sedimentary core dated) show a drop in tree pollen during the Late Neolithic/Early Chalcolithic (ca. 8–7.4 cal ka) and Late Chalcolithic/Early Bronze Age (ca. 5.7–4.6 cal ka); indeed during these periods the area was densely populated (Bottema et al., 2001).

On the basis of the pollen-anthropogenic approach (Behre, 1981) our data suggest no clear traces of human activities during the early Holocene. A similar feature is clear in other pollen profiles located near Early Neolithic settlements, where a definite sign of human presence is not found, meaning that the human activities did not strongly impact the vegetation (van Zeist and Bottema, 1991; Willis, 1995; Bottema et al., 2001). On the other hand, in the pollen record of MD01-2430 core, a deforestation phase was clearly detected

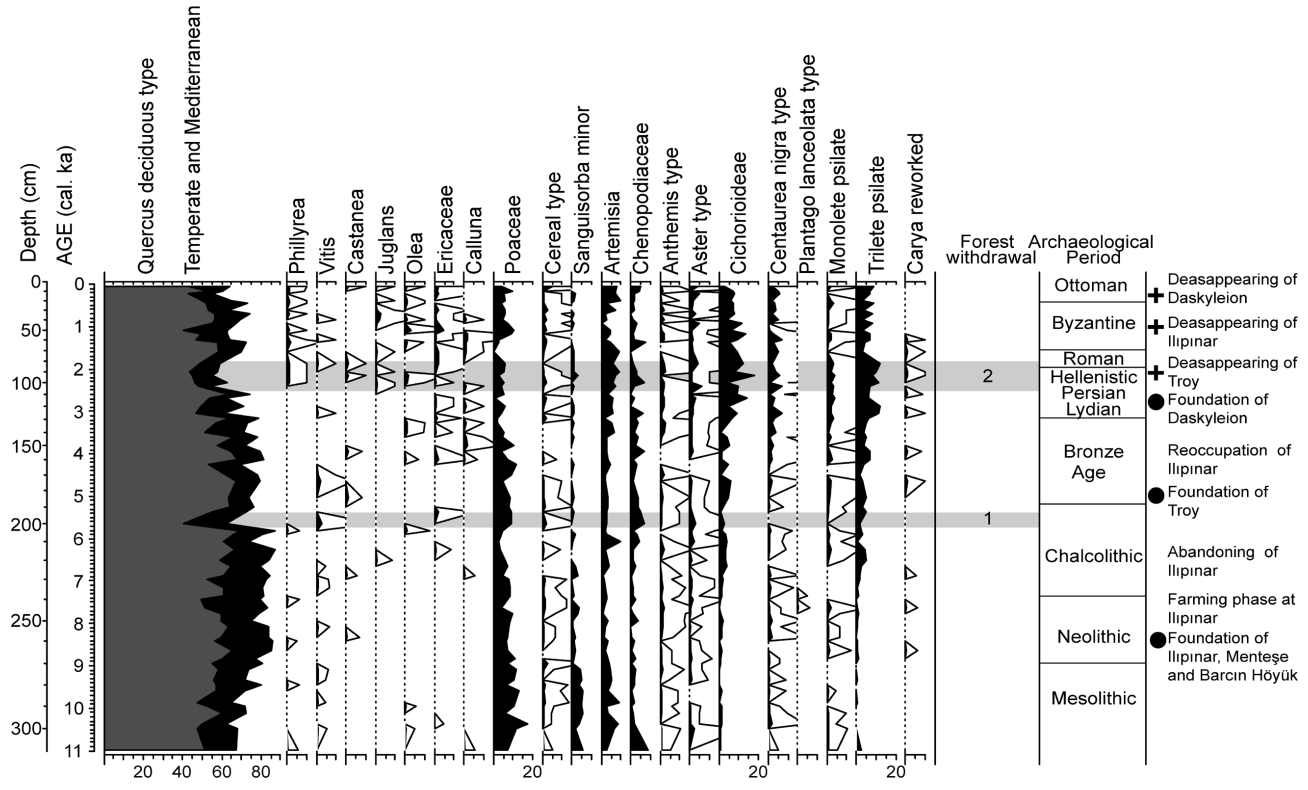


**Fig. 6.** Pollen percentage diagram showing selected taxa for core MD01-2430. Filled black curves show the percentage values of single pollen type; white curves indicate percentages enlarged by ten. Gray bands indicate phases of forest withdrawal for anomalies above 20 %. Archaeological periods and most important events in the past societies for northern Anatolia region are shown on the far right, with circles indicating foundation of settlement(s) and crosses indicating their disappearance.

at ca. 5.5 cal ka (Fig. 6). Considering chronological uncertainty, the forest setback at 5.5 cal ka might be related to the occupation phase around the nearby Illıpınar site during Late Chalcolithic/Early Bronze Age. Simultaneously, in the city of Kumtepe (ca. 5.5 cal ka) and later on in Troy (ca. 4.5 cal ka) there is clear evidence of increasing openness (Korfmann, 2006; Riehl and Marinova, 2008). However, this deforestation phase is also linked with a period of climatic deterioration (see previous section).

The presence in our pollen diagram of *Juglans*, *Olea*, *Phillyrea*, Ericaceae, Cerealia type, and *Centaurea nigra* type, as well as a steady increase of *Artemisia*, Cichorioideae, and trilete spores (possibly *Pteridium*) since ca. 2.5 cal ka, indicate a marked change in the landscape (Fig. 6). This pollen assemblage suggests an opening of the forests in correspondence to an increase of human activities (e.g. cultivation of cereals and possibly arboriculture). The ancient city of Daskyleion laid on the shore of Lake Manyas, near the south-western shore of Sea of Marmara (Fig. 1), from the Bronze Age to the Roman Period (ca. 2.6–0.3 cal ka, Leroy et al., 2002). A pollen sequence from Lake Manyas indicates an increase of pollen percentage of *Juglans*, *Castanea*, *Vitis*, *Olea*, *Fraxinus ornus*, and *Quercus* (Leroy et al., 2002), suggesting a phase of intense human occupation characterised by arboriculture (the so-called Beyşehir Occupation Phase or BOP) (van Zeist and Bottema, 1991; Leroy et al., 2002). The BOP is reflected in several pollen diagram of southwestern Turkey and it is dated from 3.5–1.4 cal ka (Eastwood et al., 1998). Although Lake Manyas lies few kilometres away from the Sea of Marmara, in our pollen diagram a clear BOP cannot be detected.

## 6 Conclusions

The marine pollen record from the Sea of Marmara, core MD01-2430, confirms the high vulnerability of the vegetation in Eastern Mediterranean (Northern Anatolia) to changes in the winter–spring precipitation regime and temperature. Steppic plants (such as *Artemisia* and Chenopodiaceae) dominated vegetation during periods with cold and dry climatic regime (e.g. HS1, YD), whereas Cichorioideae and Aster type and *Hippophaë* dominated during the LGM. We have shown a wet to dry trend within the HS1 in the Sea of Marmara region and drier and colder conditions than during the LGM, just as was found in the Western Mediterranean (Naughton et al., 2007; Fletcher et al., 2010a), confirming that western storm tracks penetrated during the LGM

as far as the Eastern Mediterranean (Kuhlemann et al., 2008; Laîné et al., 2009). Surprisingly, our record does not show a time lag during the Holocene reforestation (ca. 11.5 cal ka), pointing to the fact that northern Anatolia lies on a transitional area compared to the Near East or continental areas (see Black Sea records), where drought was a limiting factor up to 9–8 cal ka. In our record, as soon as moisture was sufficient forest vegetation expanded, probably also indicating presence of refugia of deciduous oak near the Sea of Marmara, as predicted by model simulations (Arpe et al., 2011). The anthropogenic-pollen indicators approach shows that disentangling the climate from human signals in pollen sequences in the Eastern Mediterranean is still an open issue. Contemporaneous with a major regional human occupation, the major forest-withdrawal phase at 5.5 cal ka directly associated with SST lowering episodes can be linked to periods of low temperature and to winter precipitation according to pollen-independent palaeoclimatic proxies. Consistent with several palaeoproxies in the Eastern Mediterranean, the winter rainfall regime can be related to the SH and/or NAO. Regarding the perspective of the future climate changes towards increased dry spells, a better understanding of these climatic systems could be achieved by the comparison of high-resolution palaeoproxies from Eastern and Western Mediterranean.

*Acknowledgements.* We thank Miryam Bar-Matthews, Dominik Fleitmann and Laurence Vidal for respectively providing data on oxygen isotopes of Soreq Cave, carbon isotopes of Sofular Cave and sea-surface temperatures of core MD01-2430 that are present in Figs. 4 and 5; and Fakke Gerritsen of the NIT (The Netherlands Institute in Turkey) in Istanbul for kindly providing assistance regarding data on prehistoric settlements in Anatolia. Guillemette Ménot and Laurence Vidal are acknowledged for constructive comments. We are also indebted to the three referees for valuable comments and corrections. We also thank Olga Kwiecien for discussion about the reservoir age of the Black Sea. Linguistic improvements of the manuscript by H. E. Wright Jr. are gratefully acknowledged as well as technical assistance given by Marie-Hélène Castera.

Edited by: J. Guiot


The publication of this article is financed by CNRS-INSU.

## References

Alcamo, J., Moreno, J. M., Novaky, B., Bindi, M., Corobov, R., Devoy, R. J. N., Giannakopoulos, C., Martin, E., Olesen, J. E., and Shvidenko, A.: Europe, in: Climate Change 2007: Impacts, Adaptation and Vulnerability, in: Contribution of Working Group II to the Fourth Assessment Report of the Intergovernmental Panel on Climate Change, edited by: Parry, M. P., Canziani, O. F., Palutikof, J. P., van der Linden, P. J., Hanson, C. E., Cambridge University Press, Canbridge, 541–580, 2007.

Almogi-Labin, A., Bar-Matthews, M., Shriki, D., Kolosovsky, E., Paterne, M., Schilman, B., Ayalon, A., Aizenshtat, Z., and Matthews, A.: Climatic variability during the last similar to 90 ka of the southern and northern Levantine Basin as evident from marine records and speleothems, Quaternary Sci. Rev., 28, 2882–2896, 2009.

Andersen, K. K., Svensson, A., Johnsen, S. J., Rasmussen, S. O., Bigler, M., Rothlisberger, R., Ruth, U., Siggaard-Andersen, M. L., Steffensen, J. P., Dahl-Jensen, D., Vinther, B. M., and Clausen, H. B.: The Greenland Ice Core Chronology 2005, 15–42 ka, Part 1: constructing the time scale, Quaternary Sci. Rev., 25, 3246–3257, 2006.

Arpe, K., Leroy, S. A. G., and Mikolajewicz, U.: A comparison of climate simulations for the last glacial maximum with three different versions of the ECHAM model and implications for summer-green tree refugia, Clim. Past, 7, 91–114, doi:10.5194/cp-7-91-2011, 2011.

Atanassova, J.: Palaeoecological setting of the western Black Sea area during the last 15 000 years, Holocene, 15, 576–584, 2005.

Bar-Matthews, M. and Ayalon, A.: Mid-Holocene climate variations revealed by high-resolution speleothem records from Soreq Cave, Israel and their correlation with cultural changes, Holocene, 21, 163–171, 2011.

Bar-Matthews, M., Ayalon, A., and Kaufman, A.: Late Quaternary paleoclimate in eastern Mediterranean region from stable isotope analysis of speleothems at Soreq Cave, Israel, Quaternary Res., 47, 155–168, 1997.

Bartov, Y., Goldstein, S. L., Stein, M., and Enzel, Y.: Catastrophic arid episodes in the Eastern Mediterranean linked with the North Atlantic Heinrich events, Geology, 31, 439–442, 2003.

Behre, K.-E.: The interpretation of anthropogenic indicators in pollen diagrams, Pollen et Spores, 23, 225–245, 1981.

Behre, K.-E.: Some reflections on anthropogenic indicators and the record of prehistoric occupation phases in pollen diagrams from the Near East, in: Man's Role in the Shaping of the Eastern Mediterranean Landscape, edited by: Bottema, S., Entjes-Nieborg, G., and van Zeist, W., Balkema, Rotterdam, 219–230, 1990.

Berger, A. and Loutre, M. F.: Insolation values for the climate of the last 10 million years, Quaternary Sci. Rev., 10, 297–317, 1991.

Birks, H. J. B. and Heegaard, E.: Developments in age-depth modelling of Holocene stratigraphical sequences, PAGES, 11, 7–8, 2003.

Bond, G., Showers, W., Cheseby, M., Lotti, R., Almasi, P., deMenocal, P., Priore, P., Cullen, H., Hajdas, I., and Bonani, G.: A Pervasive Millennial-Scale Cycle in North Atlantic Holocene and Glacial Climates, Science, 278, 1257–1266, 1997.

Bond, G., Kromer, B., Beer, J., Muscheler, R., Evans, M. N., Showers, W., Hoffmann, S., Lotti-Bond, R., Hajdas, I., and Bonani, G.: Persistent solar influence on North Atlantic climate during the Holocene, Science, 294, 2130–2136, 2001.

Bottema, S. and Sarpaki, A.: Environmental change in Crete: a 9000-year record of Holocene vegetation history and the effect of the Santorini eruption, Holocene, 13, 733–749, 2003.

Bottema, S. and Woldring, H.: Anthropogenic indicators in the pollen record of the Eastern Mediterranean, in: Man's Role in the Shaping of the Eastern Mediterranean Landscape, edited by: Bottema, S., Entjes-Nieborg, G., and van Zeist, W., Balkema, Rotterdam, 231–264, 1990.

Bottema, S., Woldring, H., and Kayan, I.: The late Quaternary vegetation history of western Turkey, in: The Ilipinar excavations II, edited by: Roodenberg, J. J. and Thissen, L. C., Nederlands Instituut voor het Nabije Oosten, Leiden, 327–354, 2001.

Boucher, K. (Ed.): Global climate, The English Universities Press Ltd, London, 1974.

Brayshaw, D. J., Rambeau, C. M. C., and Smith, S. J.: Changes in Mediterranean climate during the Holocene: Insights from global and regional climate modelling, Holocene, 21, 15–31, 2011.

Çağatay, M. N., Görür, N., Algan, O., Eastoe, C., Tchapalyga, A., Ongan, D., Kuhn, T., and Kusçu, I.: Late Glacial-Holocene palaeoceanography of the Sea of Marmara: timing of connections with the Mediterranean and the Black Seas, Mar. Geol., 167, 191–206, 2000.

Çağatay, M. N., Eriş, K., Ryan, W. B. F., Sancar, U., Polonia, A., Akçer, S., Biltekin, D., Gasperini, L., Görür, N., Lericolais, G., and Bard, E.: Late Pleistocene-Holocene evolution of the northern shelf of the Sea of Marmara, Mar. Geol., 265, 87–100, 2009.

Combourieu-Nebout, N., Peyron, O., Dormoy, I., Desprat, S., Beaudouin, C., Kotthoff, U., and Marret, F.: Rapid climatic variability in the west Mediterranean during the last 25 000 years from high resolution pollen data, Clim. Past, 5, 503–521, doi:10.5194/cp-5-503-2009, 2009.

Dansgaard, W., Johnsen, S. J., Clausen, H. B., Dahl-Jensen, D., Gundestrup, N. S., Hammer, C. U., Hvidbjerg, C. S., Steffensen, J. P., Sveinbjörnsdottir, A. E., Jouzel, J., and Bond, G.: Evidence for general instability of past climate from a 250-kyr ice-core record, Nature, 364, 218–220, 1993.

Djamali, M., de Beaulieu, J. L., Shah-Hosseini, M., Andrieu-Ponel, V., Ponel, P., Amini, A., Akhani, H., Leroy, S. A. G., Stevens, L., Lahijam, H., and Brewer, S.: A late Pleistocene long pollen record from Lake Urmia, NW Iran, Quarternary Res., 69, 413–420, 2008.

Djamali, M., Akhani, H., Andrieu-Ponel, V., Braconnot, P., Brewer, S., de Beaulieu, J.-L., Fleitmann, D., Fleury, J., Gasse, F., Guibal, F., Jackson, S.T., Lézine, A.-M., Médail, F., Ponel, P., Roberts, N., Stevens, L.: Indian Summer Monsoon variations could have affected the early-Holocene woodland expansion in the Near East, Holocene, 20, 813–820, 2010.

Dormoy, I., Peyron, O., Combourieu Nebout, N., Goring, S., Kotthoff, U., Magny, M., and Pross, J.: Terrestrial climate variability and seasonality changes in the Mediterranean region between 15 000 and 4000 years BP deduced from marine pollen records, Clim. Past, 5, 615–632, doi:10.5194/cp-5-615-2009, 2009.

Eastwood, W. J., Roberts, C. N., and Lamb, H. F.: Palaeoecological and archaeological evidence for human occupance in southwest Turkey: the Beysehir Occupation Phase, Anatol. Stud., 48, 69–86, 1998.

Eriksen, U., Friedrich, W. L., Buchardt, B., Tauber, H., and Thomsen, M. S.: The Stronghyle caldera: geological, palaentological and stable isotope evidence from radiocarbon-dated stromatolites from Santorini, in: Thera and the Aegean World III, Volume Two: Earth Sciences, edited by: Hardy, D. A., Keller, J., Galanopoulos, V. P., Flemming, N. C., and Druitt, T. H., The Thera Foundation, London, 139–150, 1990.

Eriş, K. K., Çağatay, M. N., Akçer, S., Gasperini, L., and Mart, Y.: Late glacial to Holocene sea-level changes in the Sea of Marmara: new evidence from high-resolution seismics and core studies, Geo.-Mar. Lett., 31, 1–18, 2011.

Finsinger, W. and Tinner, W.: Minimum count sums for charcoal-concentration estimates in pollen slides: reliability and potential errors, Holocene, 15, 293–297, 2005.

Fleitmann, D., Burns, S. J., Mangini, A., Mudelsee, M., Kramers, J., Villa, I., Neff, U., Al-Subbary, A. A., Buettner, A., Hippler, D., and Matter, A.: Holocene ITCZ and Indian monsoon dynamics recorded in stalagmites from Oman and Yemen (Socotra), Quaternary Sci. Rev., 26, 170–188, 2007.

Fleitmann, D., Cheng, H., Badertscher, S., Edwards, R. L., Mudelsee, M., Göktürk, O. M., Fankhauser, A., Pickering, R., Raible, C. C., Matter, A., Kramers, J., and Tüysüz, O.: Timing and climatic impact of Greenland interstadials recorded in stalagmites from northern Turkey, Geophys. Res. Lett., 36, L19707, doi:10.1029/2009GL040050, 2009.

Fletcher, W. J. and Sanchez Goñi, M. F.: Orbital- and sub-orbital-scale climate impacts on vegetation of the western Mediterranean basin over the last 48,000 yr, Quaternary Res., 70, 451–464, 2008.

Fletcher, W. J., Sanchez Goñi, M.F., Allen, J. R. M., Cheddadi, R., Combourieu-Nebout, N., Huntley, B., Lawson, I., Londeix, L., Magri, D., Margari, V., Muller, U. C., Naughton, F., Novenko, E., Roucoux, K., and Tzedakis, P. C.: Millennial-scale variability during the last glacial in vegetation records from Europe, Quaternary Sci. Rev., 29, 2839–2864, 2010a.

Fletcher, W. J., Sanchez Goñi, M. F., Peyron, O., and Dormoy, I.: Abrupt climate changes of the last deglaciation detected in a Western Mediterranean forest record, Clim. Past, 6, 245–264, doi:10.5194/cp-6-245-2010, 2010b.

Genty, D., Blamart, D., Ghaleb, B., Plagnes, V., Causse, C., Bakalowicz, M., Zouari, K., Chkir, N., Hellstrom, J., Wainer, K., and Bourges, F.: Timing and dynamics of the last deglaciation from European and North African $\delta^{13}$C stalagmite profiles – comparison with Chinese and South Hemisphere stalagmites, Quaternary Sci. Rev., 25, 2118–2142, 2006.

Geraga, M., Ioakim, C., Lykousis, V., Tsaila-Monopolis, S., and Mylona, G.: The high-resolution palaeoclimatic and palaeoceanographic history of the last 24,000 years in the central Aegean Sea, Greece, Paleogeogr. Paleoclimatol. Paleoecol., 287, 101–115, 2010.

Geraga, M., Tsaila-Monopolis, S., Ioakim, C., Papatheodorou, G., Ferentinos, G.: Short-term climate changes in the southern Aegean Sea over the last 48,000 years, Paleogeogr Paleoclimatol Paleoecol, 220, 311-332, 2005.

Giorgi, F. and Lionello, P.: Climate change projections for the Mediterranean region, Global Planet. Change, 63, 90–104, 2008.

Göktürk, O. M., Fleitmann, D., Badertscher, S., Cheng, H., Edwards, R. L., Leuenberger, M., Fankhauser, A., Tüysüz, O., and Kramers, J.: Climate on the southern Black Sea coast during the Holocene: implications from the Sofular Cave record, Quaternary Sci. Rev., 30, 2433–2445, 2011.

Grimm, E. C.: Tilia version 2.0 and Tilia*Graph 1.25, 1993.

Heegaard, E., Birks, H. J. B., and Telford, R. J.: Relationships between calibrated ages and depth in stratigraphical sequences: an estimation procedure by mixed-effect regression, Holocene, 15, 612–618, 2005.

Heusser, L. and Balsam, W. L.: Pollen Distribution in Northeast Pacific Ocean, Quaternary Res., 7, 45–62, 1977.

Hughen, K. A., Baillie, M. G. L., Bard, E., Warren Beck, J., Bertrand, C. J. H., Blackwell, P. G., Buck, C. E., Burr, G. S., Cutler, K. B., Damon, P. E., Edwards, R. L., Fairbanks, R. G., Friedrich, M., Guilderson, T. P., Kromer, B., McCormac, G., Manning, S., Ramsey, C. B., Reimer, P. J., Reimer, R. W., Remmele, S., Southon, J. R., Stuiver, M., Talamo, S., Taylor, F. W., van der Plicht, J., and Weyhenmeyer, C. E.: Marine04 marine radiocarbon age calibration, 0–26 cal kyr BP, Radiocarbon, 46, 1059–1086, 2004.

Jones, M. D., Roberts, C. N., and Leng, M. J.: Quantifying climatic change through the last glacial–interglacial transition based on lake isotope palaeohydrology from central Turkey, Quaternary Res., 67, 463–473, 2007.

Kazancı, N., Leroy, S., Ileri, Ö., Emre, Ö., Kibar, M., and Öncel, S.: Late Holocene erosion in NW Anatolia from sediments of Lake Manyas, Lake Ulubat and the southern shelf of the Marmara Sea, Turkey, Catena, 57, 277–308, 2004.

Köppen, W. (Ed.): Die Klimate der Erde, Grundriss der Klimakunde, Der Gruyter, Berlin, 1923.

Korfmann, M. (Ed.): Troia – Archäologie eines Siedlungshügels und seiner Landschaft, P. von Zabern, Mainz am Rhein, 2006.

Kotthoff, U., Muller, U. C., Pross, J., Schmiedl, G., Lawson, I. T., van de Schootbrugge, B., and Schulz, H.: Lateglacial and Holocene vegetation dynamics in the Aegean region: an integrated view based on pollen data from marine and terrestrial archives, Holocene, 18, 1019–1032, 2008a.

Kotthoff, U., Pross, J., Muller, U. C., Peyron, O., Schmiedl, G., Schulz, H., and Bordon, A.: Climate dynamics in the borderlands of the Aegean Sea during formation of sapropel S1 deduced from a marine pollen record, Quaternary Sci. Rev., 27, 832–845, 2008b.

Kotthoff, U., Koutsodendris, A., Pross, J., Schmiedl, G., Bornemann, A., Kaul, C., Marino, G., Peyron, O., and Schiebel, R.: Impact of Lateglacial cold events on the northern Aegean region reconstructed from marine and terrestrial proxy data, J. Quaternary Sci., 26, 86–96, 2011.

Kuhlemann, J., Rohling, E. J., Krumrei, I., Kubik, P., Ivy-Ochs, S., and Kucera, M.: Regional synthesis of Mediterranean atmospheric circulation during the last glacial maximum, Science, 321, 1338–1340, 2008.

Kwiecien, O., Arz, H. W., Lamy, F., Wulf, S., Bahr, A., Rohl, U., and Haug, G. H.: Estimated reservoir ages of the Black Sea since the last glacial, Radiocarbon, 50, 99–118, 2008.

Laîné, A., Kageyama, M., Salas-Mélia, D., Voldoire, A., Rivière, G., Ramstein, G., Planton, S., Tyteca, S., and Peterschmitt, J.: Northern hemisphere storm tracks during the last glacial maximum in the PMIP2 ocean-atmosphere coupled models: energetic study, seasonal cycle, precipitation, Clim. Dynam., 32, 593–614, 2009.

Lamy, F., Arz, H. W., Bond, G. C., Bahr, A., and Patzold, J.: Multicentennial-scale hydrological changes in the Black Sea and northern Red Sea during the Holocene and the Arctic/North Atlantic oscillation, Paleoceanography, 21, Pa1008, doi:10.1029/2005pa001184, 2006.

Lawson, I. T., Al-Omari, S., Tzedakis, P. C., Bryant, C. L., and Christanis, K.: Lateglacial and Holocene vegetation history at Nisi Fen and the Boras mountains, northern Greece, Holocene, 15, 873–887, 2005.

Leroy, S., Kazanci, N., Ileri, O., Kibar, M., Emre, O., McGee, E., and Griffiths, H. I.: Abrupt environmental changes within a late Holocene lacustrine sequence south of the Marmara Sea (Lake Manyas, N-W Turkey): possible links with seismic events, Mar. Geol., 190, 531–552, 2002.

Leroy, S. A. G. and Arpe, K.: Glacial refugia for summer-green trees in Europe and south-west Asia as proposed by ECHAM3 time-slice atmospheric model simulations, J. Biogeogr., 34, 2115–2128, 2007.

Leroy, S. A. G., Boyraz, S., and Gürbüz, A.: High-resolution palynological analysis in Lake Sapanca as a tool to detect recent earthquakes on the North Anatolian Fault, Quaternary Sci. Rev., 28, 2616–2632, 2009.

Londeix, L., Herreyre, Y., Turon, J.-L., and Fletcher, W.: Last Glacial to Holocene hydrology of the Marmara Sea inferred from a dinoflagellate cyst record, Rev. Palaeobot. Palynol., 158, 52–71, 2009.

Maher, L. J.: Nomograms for computing 0.95 confidence limits of pollen data, Rev. Palaeobot. Palynol., 32, 153–191, 1981.

Marino, G., Rohling, E. J., Sangiorgi, F., Hayes, A., Casford, J. L., Lotter, A. F., Kucera, M., and Brinkhuis, H.: Early and middle Holocene in the Aegean Sea: interplay between high and low latitude climate variability, Quaternary Sci. Rev., 28, 3246–3262, 2009.

Mayewski, P. A., Meeker, L. D., Twickler, M. S., Whitlow, S., Yang, Q. Z., Lyons, W. B., and Prentice, M.: Major features and forcing of high-latitude northern hemisphere atmospheric circulation using a 110,000-year-long glaciochemical series, J. Geophys. Res.-Oceans, 102, 26345–26366, 1997.

Mix, A. C., Bard, E., and Schneider, R.: Environmental processes of the ice age: land, oceans, glaciers (EPILOG), Quaternary Sci. Rev., 20, 627–657, 2001.

Moore, P. D., Webb, J. A., and Collinson, M. E. (Eds.): Pollen Analysis, Blackwell Scientific Publications, London, 1991.

Mudie, P. J., Rochon, A., Aksu, A. E., and Gillespie, H.: Dinoflagellate cysts, freshwater algae and fungal spores as salinity indicators in Late Quaternary cores from Marmara and Black seas, Mar. Geol., 190, 203–231, 2002.

Mudie, P. J., Marret, F., Aksu, A. E., Hiscott, R. N., and Gillespie, H.: Palynological evidence for climatic change, anthropogenic activity and outflow of Black Sea water during late Pleistocene and Holocene: Centennial- to decadal-scale records from the Black and Marmara Seas, Quatern. Int., 167, 73–90, 2007.

Naughton, F., Goni, M. F. S., Desprat, S., Turon, J. L., Duprat, J., Malaize, B., Joli, C., Cortijo, E., Drago, T., and Freitas, M. C.: Present-day and past (last 25 000 years) marine pollen signal off western Iberia, Mar. Micropaleontol., 62, 91–114, 2007.

Özdogan, M.: Eastern Thrace the contact zone between Anatolia and the Balkans, in: The Oxford Handbook of Anatolian Studies (10000-323 BCE), edited by: Steadman, S. and McMahon, G., Oxford University Press, Oxford, UK, 898–923, 2011.

Pichler, H. and Friedrich, W.: Radiocarbon dates of santorini volcanics, Nature, 262, 373–374, 1976.

Pross, J., Kotthoff, U., Müller, U. C., Peyron, O., Dormoy, I., Schmiedl, G., Kalaitzidis, S., and Smith, A. M.: Massive perturbation in terrestrial ecosystems of the Eastern Mediterranean region associated with the 8.2 kyr BP climatic event, Geology, 37, 887–890, 2009.

Rasmussen, S. O., Andersen, K. K., Svensson, A. M., Steffensen, J. P., Vinther, B. M., Clausen, H. B., Siggaard-Andersen, M.-L., Johnsen, S. J., Larsen, L. B., Dahl-Jensen, D., Bigler, M., Röthlisberger, R., Fischer, H., Goto-Azuma, K., Hansson, M. E., and Ruth, U.: A new Greenland ice core chronology for the last glacial termination, J. Geophys. Res.-Atmos., 111, D06102, doi:10.1029/2005JD006079, 2006.

Reille, M. (Ed.): Pollen et spores d'Europe et d'Afrique du nord, Supplement 1 and 2, Laboratoire de Botanique hostorique et Palynologie, Marseille, 1992–1998.

Reimer, P. J., Baillie, M. G. L., Bard, E., Bayliss, A., Warren Beck, J., Bertrand, C. J. H., Blackwell, P. G., Buck, C. E., Burr, G. S., Cutler, K. B., Damon, P. E., Lawrence Edwards, R., Fairbanks, R. G., Friedrich, M., Guilderson, T. P., Hogg, A. G., Hughen, K. A., Kromer, B., McCormac, G., Manning, S., Ramsey, C. B., Reimer, R. W., Remmele, S., Southon, J. R., Stuiver, M., Talamo, S., Taylor, F. W., van der Plicht, J., and Weyhenmeyer, C. E.: IntCal04 terrestrial radiocarbon age calibration, 0–26 cal kyr BP, Radiocarbon, 46, 1029–1058, 2004.

Riehl, S. and Marinova, E.: Mid-Holocene vegetation change in the Troad (W Anatolia): man-made or natural?, Veg. Hist. Archaeobot., 17, 297–312, 2008.

Roberts, N. and Wright Jr., H. E.: Vegetational, lake-level, and climatic history of the Near East and southwest Asia, in: Global climates since the past Last Glacial Maximum, edited by: Wright, H. E. J., Kutzbach, J. E., Webb III, T., Ruddiman, W. F., Street-Perrott, F. A., and Bardein, P. J., University of Minneapolis Press, Minneapolis, 194–220, 1993.

Roberts, N., Reed, J. M., Leng, M. J., Kuzucuoğlu, C., Fontugne, M., Bertaux, J., Woldring, H., Bottema, S., Black, S., Hunt, E., and Karabıyıkoğlu, M.: The tempo of Holocene climatic change in the eastern Mediterranean region: new high-resolution crater-lake sediment data from central Turkey, Holocene, 11, 721–736, 2001.

Roberts, N., Eastwood, W. J., Kuzucuoğlu, C., Fiorentino, G., and Caracuta, V.: Climatic, vegetation and cultural change in the eastern Mediterranean during the mid-Holocene environmental transition, Holocene, 21, 147–162, 2011.

Roberts, N., Moreno, A., Valero-Garcés, B. L., Corella, J. P., Jones, M., Allcock, S., Woodbridge, J., Morellón, M., Luterbacher, J., Xoplaki, E., and Türkeş, M.: Palaeolimnological evidence for an east–west climate see-saw in the Mediterranean since AD 900, Global Planet. Change, 84–85, 23–34, 2012.

Rohling, E. J., Mayewski, P. A., Abu-Zied, R. H., Casford, J. S. L., and Hayes, A.: Holocene atmosphere-ocean interactions: records from Greenland and the Aegean Sea, Clim. Dynam., 18, 587–593, 2002.

Roodenberg, J. J. and Alpaslan-Roodenberg, S.: The Neolithic in the eastern Marmara: two examples of settlement, in: Neolithic in Turkey, edited by: Ozdogan, M. and Basgelen, N., Arkeoloji ve Sanat Yayinlari, Istanbul, 1–7, 1999.

Rosenstock, E.: Höyük, Toumba and Mogila: a settlement form in Anatolia and the Balkans and its ecological determination 6500–5500 BC, in: How did farming reach Europe?, edited by: Lichter, C., Bizas, 2, 221–237, 2005.

Rossignol-Strick, M.: Sea-land correlation of pollen records in the Eastern Mediterranean for the glacial-interglacial transition: Biostratigraphy versus radiometric time-scale, Quaternary Sci. Rev., 14, 893–915, 1995.

Rossignol-Strick, M. and Planchais, N.: Climate patterns revealed by pollen and oxygen isotope records of a Tyrrhenian sea core, Nature, 342, 413–416, 1989.

Rull, V.: A note on pollen counting in palaeoecology, Pollen et Spores, 29, 471–480, 1987.

Saaroni, H., Bitan, A., Alpert, P., and Ziv, B.: Continental Polar outbreaksinto the Levant and Eastern Mediterranean, Int. J. Climatol., 16, 1175–1191, 1996.

Sanchez Goñi, M. F. and Harrison, S. P.: Millennial-scale climate variability and vegetation changes during the Last Glacial: Concepts and terminology, Quaternary Sci. Rev., 29, 2823–2827, 2010.

Shumilovskikh, L. S., Tarasov, P., Arz, H. W., Fleitmann, D., Marret, F., Nowaczyk, N., Plessen, B., Schlütz, F., and Behling, H.: Vegetation and environmental dynamics in the southern Black Sea region since 18 kyr BP derived from the marine core 22-GC3, Paleogeogr. Paleoclimatol. Paleoecol., 337–338, 177–193, 2012.

Siani, G., Paterne, M., Arnold, M., Bard, E., Métivier, B., Tisnerat, N., Bassinot, F.: Radiocarbon reservoir ages in the Mediterranean Sea and Black Sea, Radiocarbon, 42, 271-280, 2000.

Stanford, J. D., Rohling, E. J., Bacon, S., Roberts, A. P., Grousset, F. E., and Bolshaw, M.: A new concept for the paleoceanographic evolution of Heinrich event 1 in the North Atlantic, Quaternary Sci. Rev., 30, 1047–1066, 2011.

Steffensen, J. P., Andersen, K. K., Bigler, M., Clausen, H. B., Dahl-Jensen, D., Fischer, H., Goto-Azuma, K., Hansson, M., Johnsen, S. J., Jouzel, J., Masson-Delmotte, V., Popp, T., Rasmussen, S. O., Röthlisberger, R., Ruth, U., Stauffer, B., Siggaard-Andersen, M.-L., Sveinbjörnsdóttir, À., Svensson, A., and White, J. W. C.: High-Resolution Greenland Ice Core Data Show Abrupt Climate Change Happens in Few Years, Science, 321, 680–684, 2008.

Stevens, L. R., Wright Jr., H. E., and Ito, E.: Proposed changes in seasonality of climate during the Lateglacial and Holocene at Lake Zeribar, Iran, Holocene, 11, 747–755, 2001.

Stevens, L. R., Ito, E., Schwalb, A., and Wright Jr., H. E.: Timing of atmospheric precipitation in the Zagros Mountains inferred from a multi-proxy record from Lake Mirabad, Iran, Quaternary Res., 66, 494–500, 2006.

Stockmarr, J.: Tablets with spores used in absolute pollen analysis, Pollen et Spores, 13, 614–621, 1971.

Stuiver, M., Reimer, P. J., Bard, E., Beck, J. W., Burr, G. S., Hughen, K. A., Kromer, B., McCormac, F. G., van der Plicht, J., and Spurk, M.: INTCAL98 Radiocarbon Age Calibration, 24,000–0 cal BP, Radiocarbon, 40, 1041–1083, 1998.

Trewartha, G. T. (Ed.): The Earth's problem climates, The University of Wisconsin Press, Madison, 1981.

Turner, C. and Sánchez Goñi, M.-F.: Late glacial landscape and vegetation in Epirus, in: Klithi: Palaeolithic Settlement and Quaternary Landscapes in Northwest Greece, edited by: Bailey, G., McDonald Institute for Archaeological Research, Cambridge, 559–585, 1997.

Turon, J. L.: Direct Land Sea Correlations in the Last Interglacial Complex, Nature, 309, 673–676, 1984.

Tzedakis, P. C.: Seven ambiguities in the Mediterranean palaeoenvironmental narrative, Quaternary Sci. Rev., 26, 2042–2066, 2007.

Tzedakis, P. C., Frogley, M. R., Lawson, I. T., Preece, R. C., Cacho, I., and de Abreu, L.: Ecological thresholds and patterns of millennial-scale climate variability: The response of vegetation in Greece during the last glacial period, Geology, 32, 109–112, 2004.

Ünlüata, Ü., Öguz, T., Latif, M., and Ozsoy, E.: On the physical oceanography of the Turkish Straits, in: The Physical Oceanography of Sea Straits, NATO ASI Ser., Ser. C, vol. 318, edited by: Pratt, L. J., Kluwer Accademy, Dordrecht, 1990.

Unal, Y., Kindap, T., and Karaka, M.: Redefining the climate zones of Turkey using cluster analysis, Int. J. Climatol., 23, 1045–1055, 2003.

van Zeist, W. and Bottema, S.: Late Quaternary vegetation of the Near East, Dr. Ludwig Reichert Verlag, Wiesbaden, 1991.

Vermoere, M., Bottema, S., Vanhecke, L., Waelkens, M., Paulissen, E., and Smets, E.: Palynological evidence for late-Holocene human occupation recorded in two wetlands in SW Turkey, Holocene, 12, 569–584, 2002.

Vidal, L., Ménot, G., Joly, C., Bruneton, H., Rostek, F., Çagatay, M. N., Major, C., and Bard, E.: Hydrology in the Sea of Marmara during the last 23 ka: Implications for timing of Black Sea connections and sapropel deposition, Paleoceanography, 25, PA1205, doi:10.1029/2009PA001735, 2010.

Vinther, B. M., Clausen, H. B., Johnsen, S. J., Rasmussen, S. O., Andersen, K. K., Buchardt, S. L., Dahl-Jensen, D., Seierstad, I. K., Siggaard-Andersen, M.-L., Steffensen, J. P., Svensson, A., Olsen, J., and Heinemeier, J.: A synchronized dating of three Greenland ice cores throughout the Holocene, J. Geophys. Res.-Atmos., 111, D13102, doi:10.1029/2005JD006921, 2006.

Weiss, H., Courty, M.-A., Wetterstrom, W., Guichard, F., Senior, L., Meadow, R., and Curnow, A.: The genesis and collapse of Third Millennium North Mesopotamian civilization, Science, 261, 995–1004, 1993.

Wick, L., Lemcke, G., and Sturm, G.: Evidence of Lateglacial and Holocene climatic change and human impact in eastern Anatolia: high-resolution pollen, charcoal, isotopic and geochemical records from the laminated sediments of Lake Van, Turkey, Holocene, 13, 665–675, 2003.

Wijmstra, T. A.: Palynology of the first 30 meters of a 120 m deep section in Northern Greece, Acta Bot. Neerl., 18, 511–527, 1969.

Willis, K. J.: The pollen-sedimentological evidence for the beginning of agriculture in Southeastern Europe and Anatolia, Porocilo o raziskovanju paleolitika, neolitika in eneolitika v Sloveniji, 22, 9–24, 1995.

Wright Jr., H. E., Ammann, B., Stefanova, I., Atanassova, J., Margalitadze, N., Wick, L., and Blyakharchuk, T.: Late-glacial and Early-Holocene dry climates from the Balkan Peninsula to Southern Siberia, in: Aspects of Palynology and Palaeoecology, edited by: Tonkov, S., Pensoft, Sofia, Moscow, 127–136, 2003.

Wulf, S., Kraml, M., Kuhn, T., Schwarz, M., Inthorn, M., Keller, J., Kuscu, I., and Halbach, P.: Marine tephra from the Cape Riva eruption (22 ka) of Santorini in the Sea of Marmara, Mar. Geol., 183, 131–141, 2002.

Zohary, M. (Ed.): Geobotanical foundations of the Middle East, 2 Volumes, Gustav Fischer Verlag and Swets & Zeitlinger, Stuttgart, Amsterdam, 1973.